A Prediction model of relativistic electrons at geostationary orbit using the EMD-LSTM network and geomagnetic indexes

H. Zhang[1] H. R. Xu[1] G.S. Peng[1] Y. D. Qian[1] C. Shen[2] Z. Li[1] J. W. Yang[1] F. He[3]

[1]Institute of Space Weather, Nanjing University of Information Science & Technology, Nanjing, China.

[2]Harbin Institute of Technology, Shen Zhen, China.

[3]NMR Key laboratory for Polar Science, Polar Research Institute of China, Shang Hai, China.

Corresponding author: Hua Zhang (289534957@qq.com)

Key Points:

- Propose a prediction model of relativistic electrons using a deep learning algorithm, the EMD-LSTM model, to predict the >2MeV electron fluxes.
- Use the ultralow frequency Pc5 power and related geomagnetic indexes as input parameters to predict the >2MeV electron fluxes.
- The accuracy of storm-time forecasting is greatly improved, especially few time offset of between the observation value and the forecast value at the inflection point of lowest flux.

Abstract:

In this study, We construct the EMD-LSTM model, combined the Empirical Mode Decomposition algorithm (EMD) and the Long Short Term Memory neural network (LSTM), to predict the variation of the >2MeV electron fluxes. The Pc5 power and related geomagnetic indexes as input parameters are used to predict the >2MeV electron fluxes. Compared the prediction results of the model with other classical prediction models, the results shows that the one-day ahead prediction efficiency of the > 2MeV electron fluxes is above 0.80, and the highest prediction efficiency can reach 0.92 in 2011-2013, which is much better than the prediction result of classical prediction models. Selected two high-energy electron flux storm events to verify, the results indicates that the performance of the EMD-LSTM model in the period of the high-energy electron flux storm is also relatively good, especially for the

prediction of high-energy electron fluxes at extreme points, and the prediction is closer to actual observation.

Plain Language Summary:

During the recovery of a magnetic storm, the relativistic electron fluxes at MeV energy from the outer radiation belt will be enhanced at geosynchronous orbit. In particular, the >2MeV electrons could penetrates the surface of satellites and accumulate inside. After a long period, the effect of such electron fluxes could result in satellites to be unable to operate or to be damaged completely. A new neural network, called EMD-LSTM, is established by combination of the EMD and the LSTM, which can process the influence of non-stationary and long term non-linear of data series. The prediction results of the EMD-LSTM model is also excellent in dramatic change of data series, and particularly the extreme points of data series is accurately predicted, and few time offset.

1. Introduction

The Geosynchronous orbit (GEO) is located in the region of the outer radiation belt which distributes generous relativistic electrons. At the same time, hundreds of satellites operate in this region. During recovery phase of a magnetic storm period, the relativistic electrons rise in count from 10 up to 10^5 (electrons Sr^{-1} s^{-1}) (Sakaguchi et al., 2013). The deep-dielectric charging by relativistic electrons could damage satellites at GEO and pose a risk for space security (Wrenn et al., 2002). According to the statistics of faults, more than fifty failures of GEO satellites are caused by the accumulation of high-energy charged particles occurred from March 1992 to April 1994 (He et al., 2013). Therefore, the prediction of >2 MeV electron fluxes has important scientific and application value, which is the necessary measure to be taken in advance to reduce the harm of relativistic electrons to space instruments.

The sudden acceleration of relativistic electrons is responsible for the increase in fluxes. At present, two types of acceleration mechanism of relativistic electrons have been proposed: the mechanism of radial diffusion (Li et al., 2001)and the local interaction of wave-particle (Simms et al., 2018). Based on the radial diffusion mechanism, Li et al. (2001) proposed a radial diffusion model that takes solar wind parameters and the interplanetary magnetic field as input parameters to predict the relativistic electron fluxes of the 1-2 day ahead. The

prediction efficiency (PE) of the radial diffusion model is up to 0.64, however, that is not ideal during the solar maximum period. Turner & Li (2008) developed the LOW-E model, which uses the low-energy electron fluxes as an input parameter to predict the relativistic electron fluxes of the 1 day ahead, and the PE of that is up to 0.73. The Space Weather Prediction Center of the National Oceanic and Atmospheric Administration (NOAA), USA, developed a prediction model of relativistic electron fluxes (REFM). The REFM model uses the solar wind speed as an input parameter and provides forecasting values of >2MeV electron fluxes of the 1-3 day ahead. The prediction efficiency of the first day is 0.71, but that of the next days is poor because the outer radiation belt is rapidly variation in a magnetic disturbance period (Baker et al., 1990).

Based on the wave-particle interaction mechanism, He et al. (2013) takes geomagnetic pulsation parameters as input parameters, and combines linear filter technology and Kalman filter to establish the relativistic electrons prediction model at the GEO. The PE of model for 2004 is about 0.73, which is equivalent to the imitation REFM model. But, the prediction results is lower than other models in 2005, that PE is about 0.62. Potapov et al. (2014, 2016) combined the mechanisms of radial diffusion and wave-particle interaction to establish a daily prediction model using a multivariate regression method. This model takes the amplitude of Pc4-5 oscillation, the maximum for a day fluxes of seed electrons, and the IMF as input parameters to establish the model. The model is obviously characterized by an extreme prediction value ahead of the measured value.

ULF Pc5 waves can migrate inward to lower L-shells and may accelerate low and medium energy electrons to relativistic energy via several proposed mechanisms (Simms et al., 2018). So, the Pc5 wave may be the key to electronic excitation at GEO. There are many studies show that Pc5 power has a good correlation with relativistic electrons fluxes (Regi et al., 2015; Lam, 2017). In this work, we use Pc5 power as one of parameters to predict the > 2MeV electron fluxes.

Since the relationship between the relativistic electron fluxes and each parameter is not completely linear, the variation of relativistic electrons is too complex to describe the relationship between the input parameters and the output of electron fluxes as a functional

relationship. However, the neural network method has good learning ability and represents a better approach to solve the nonlinear problem. Fukata et al. (2002) and Ling et al. (2010) established a neural network model to predict the relativistic electron fluxes. The PE of Fukata's model is approximately 0.6. Ling's model is more efficient than Fukata's, and the PE of the model is close to 0.7, that of input parameters are the indexes of geomagnetic disturbance, however, ignored solar wind parameters. For the sudden enhancement and loss of high-energy electron fluxes, Qian et al. (2020) combined the EMD algorithm and Kalman filter algorithm to establish the EMD-KLM model for high-energy electron prediction. The average PE of > 2Mev electron fluxes can reach up to 0.8. Especially, the accuracy of forecast is excellent for the sudden decline of electron fluxes, but the accuracy of forecast needs to be improved during the sudden jump of electron fluxes.

With the development of machine learning, deep learning neural networks are also used in the prediction of high-energy electron fluxes. Wei et al. (2018) established a prediction model based on the deep learning algorithm LSTM network, called the LSTM-FRK model. The prediction efficiency of Wei’s model is in the range of 0.65-0.81, and it verifies the good effectiveness of the LSTM network in predicting high-energy electron fluxes. However, the model uses historical high-energy electron fluxes, Kp index, and daily average distances from the magnetosphere to model, which indicates that input parameters need to be further optimized. In addition, intelligent algorithms, including radial basis functions and support vector machines, are also used for the prediction of relativistic electrons (Xue & Ye, 2004; Guo et al., 2013).

Although these models have achieved great success in predicting electron fluxes, there is still much room of improvement for the accuracy of the magnetic storm period and the prediction of the minimum inflection point of the >2MeV electron fluxes. Therefore, using geomagnetic pulsation parameters and related geomagnetic indexes, we propose a new combination model, named the EMD-LSTM model, to predict the >2MeV electron fluxes based on the combination of EMD and LSTM network. The EMD-LSTM model can solve the non-stationary and nonlinear problems of high-energy electron fluxes data, and geomagnetic pulsation parameters are easier to obtain and more stable than solar wind

parameters.

2. Data

2.1 Data Source and Processing

In this work, we use a daily value of the >2 MeV electron fluxes in order to eliminate the local time effects. The fluxes data derives from the relativistic electron fluxes of 5 min time resolution is obtained from the GOES10 satellite and can be available at the NOAA website (https://satdat.ngdc.noaa.gov/sem/goes/data). The daily Pc5 power datasets derives from ground magnetic data, which is collected by CANMOS observatories located in the auroral zone proximal to footprints of field lines, and the detail of the datasets is shown in Table1. To process the magnetic data, the band pass filter is first used to filter the tiny data to extract the variation of the Pc5 band. Then, use the Hanning window to calculate the fast Fourier transform to obtain the Pc5 power spectrum estimation based on the hourly data. Finally, the hourly power is integrated to obtain daily Pc5 power.

Table1. Coordinates of CANMOS Auroral Zone Observatories

Code	Station	Geographic Latitude	Geographic Longitude	Geomagnetic Latitude	Geomagnetic Longitude	L
FCC	ForChurchill	$58.8^{\circ}N$	$94.1^{\circ}W$	$68.8^{\circ}N$	$94.1^{\circ}W$	8.18

2.2 Selection of Input Parameters

The previous studies indicated that Pc5 wave have strong correlation with energy electron fluxes increase at GEO (O'Brien et al., 2003; Borovsky & Deton, 2014; Regi et al., 2015; Lam, 2017; Simms et al., 2018). In fact, Simms et al. (2018) suggested that Pc5 waves is the main waves that drive electron acceleration. Lam (2017) analyzed the relationship between Pc5 wave and >2MeV electron fluxes in two solar cycles, and proposed that strong ground Pc5 is a precursor of enhanced relativistic electron fluxes at GEO by ahead 2-3 days for all phases. On the other hand, solar wind parameters are usually used in the prediction model of relativistic electron fluxes. Regi et al. (2015) proposes that the Pc5 power is highly correlation with solar wind pressure fluctuations and with the solar wind speed by several

hours offset. Comparison with solar wind parameters, the Pc5 power is derived from ground magnetic data, so it cost lower and is more stable than satellite data. So, we use the Pc5 power as one of input parameters to predict > 2MeV electron fluxes.

In this work, we also use the >0.6 MeV electron fluxes (Potapov et al., 2016), geomagnetic indexes (Ap, Kp, AE) (Yousrfi et al., 2009, Sakaguchi et al., 2013) and the historical >2 MeV electron fluxes (X) as other input parameters to predict the >2 MeV electron fluxes 1 day ahead. Meanwhile, analyze the correlations between each input parameter and >2MeV electron fluxes. The result is shown in Figure1.

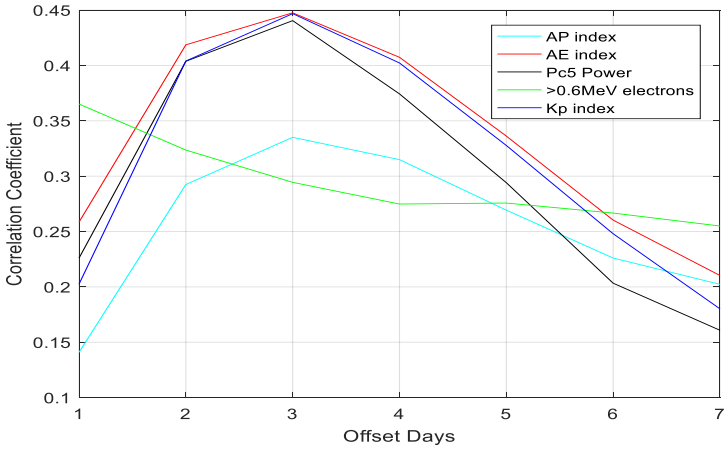

Figure1 The correlations of between input parameters used and >2MeV electron fluxes.

In Figure1, we can conclude that the best correlation of between each input and the >2MeV electron fluxes is 1-3 days ahead. So, the input parameters used in this work is shown in Table2.

Table2. The input parameters of the EMD-LSTM model

Inputs	Correlation coefficient
$Ap(t-3)$	0.33
$AE(t-3)$	0.46
$>0.6MeV(t-1)$	0.36
$Pc5(t-3)$	0.43

$Pc5(t-2)$	0.40
$Kp(t-3)$	0.44
$X(t-1)$	0.81

3. Method

3.1 EMD Algorithm

Due to the external squeeze of the solar wind, the high-energy electrons during a magnetic storm change very drastically. The non-stationary and nonlinear characteristics of the >2MeV electron fluxes data series is very obvious, which introduces great difficulties to accurate forecasting. Previous models use statistical methods to deal with the impact of nonlinear problems on forecast (Xiao et al., 2012), but the non-stationary problem of data series is not taken seriously. The EMD algorithm is a method that can well deal with the non-stationarity problem of high-energy electron flux data series, and the basic idea is that all complex signals are composed of simple eigenmode functions (IMF) (Huang et al., 1998). These IMF components are arranged in the order of high frequency to low frequency, where each IMF is independent of each other (Sain & Stephan, 1997). The components of different scales in the high-energy electron flux data sequence is decomposed one by one by the EMD algorithm, and several data sequences with different characteristic scales are generated. These components of different characteristic scales are more regular than the original high-energy electron flux data sequence, that help to improve the prediction accuracy. Qian et al. (2020) introduced the EMD algorithm to process and forecast the >2MeV electron fluxes, called the EMD-KLM model, and found that the forecast results is greatly improved comparison with the prediction result of no the EMD algorithm.

3.2 LSTM Network

The high-energy electron flux usually increases significantly during the recovery phase of a magnetic storm, and sometimes it suddenly increases by 3-4 orders of magnitude. Most of the existing forecasting models is difficult to accurately follow the event of sudden increase

in high-energy electron fluxes. However, with the development of machine learning (ML), deep learning neural networks is also used in the prediction of the >2MeV electron fluxes.

The LSTM Network is a type of recurrent neural network(RNN). The iterative function loops is used by RNN to store information (Graves, 2012). They behave as loops, allowing information to pass from one unit of the network to the next. If this loop is unrolled, the RNN would be thought as multiple copies of the same network. This feature makes RNN can remember historical information (Tan et al., 2018). Thus, it is suitable to forecast the >2MeV electron fluxes during a magnetic storm period.

However, if the information needed is too far in the past, the standard RNN is unable to learn how to connect the information each other. This problem is because of the vanishing gradient problem occurring during the training phase of RNN (Hochreiter & Schmidhuber, 1990). The LSTM is designed to avoid the vanishing gradient problem, that can remember information for long periods of time. They have a chain-like structure like RNN, but the repeating module has a specific structure. Figure 2 shows an LSTM cell. The key of the LSTM cell is as follows: 1. The cell state, and 2. The cell gate. The cell gate in green on figure 2 is like a conveyor belt which is connected to gates. Gates can add or remove information from the cell state depending on information required by the cell. Basically, three gates are used: an input gate in blue, a forget gate in purple and an output gate in red in Figure 2. The detail algorithm is described in Wei et al. (2018).

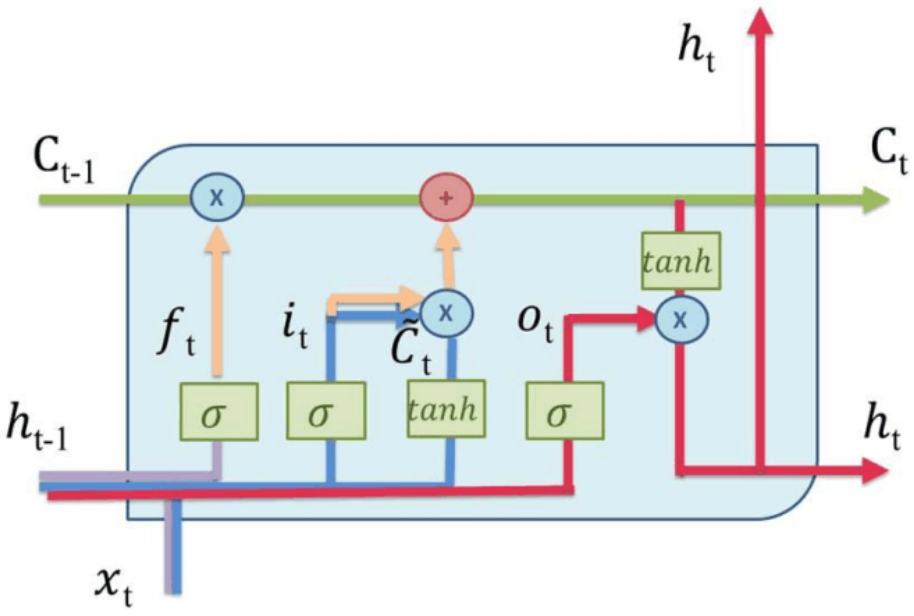

Figure 2 LSTM cell of schematic diagram. The cell state is in green, the forget in purple, the input gate in blue, and the output gate in red.

The LSTM network can more easily capture the non-linear relationship in the data set of high-energy electron flux to predict the >2 MeV electron fluxes more accurately based on the useful information in the historical data series.

Wei et al (2018) used the LSTM network to predict the daily integral values of the high-energy electron fluxes at GEO for the next day by inputting the historical high-energy electron flux, the geomagnetic index Kp, and the daily average value of the magnetopause. And the forecast results is better, which verifies the feasibility of using the LSTM network to predict the >2 MeV electron fluxes. However, the model can be further improved in the selection of predictors.

3.3 EMD-LSTM Model

The LSTM network is effective in dealing with the nonlinear problem of the data sequences. It has a memory function and can capture more complex nonlinear relationships in the data sets, which is more suitable for the prediction of the data sequences. At the same time, the EMD algorithm is very effective in dealing with the non-stationary problem of high-energy electron flux data series. Therefore, we combine the EMD algorithm and the LSTM network to predict the >2 MeV electron fluxes at GEO for the first time. The combined forecast model is named the EMD-LSTM model, which uses ultra-low frequency Pc5 power as one of input parameters to predict the >2 MeV electron fluxes.

Figure 3 shows the main process of the combined forecast. The main steps is as follows:

(1) Use the EMD algorithm to decompose the observed values of the >2 MeV electron fluxes to obtain n IMF components and one margin;

(2) Input the prepared predictor into the LSTM network；

(3) Use the LSTM network to predict each component and get the predicted value of each component for the next day;

(4) Add the predicted values of n components to obtain the predicted value of the > 2MeV electron fluxes for the next day;

The EMD-LSTM model is a rolling forecast model, so the data sets needs to be re-decomposed in advance every day for the next forecast. The time step of the combined forecasting model is 3 steps and it means that the daily flux of the >2 MeV electron fluxes for the next day is predicted by the historical data of the previous three days.

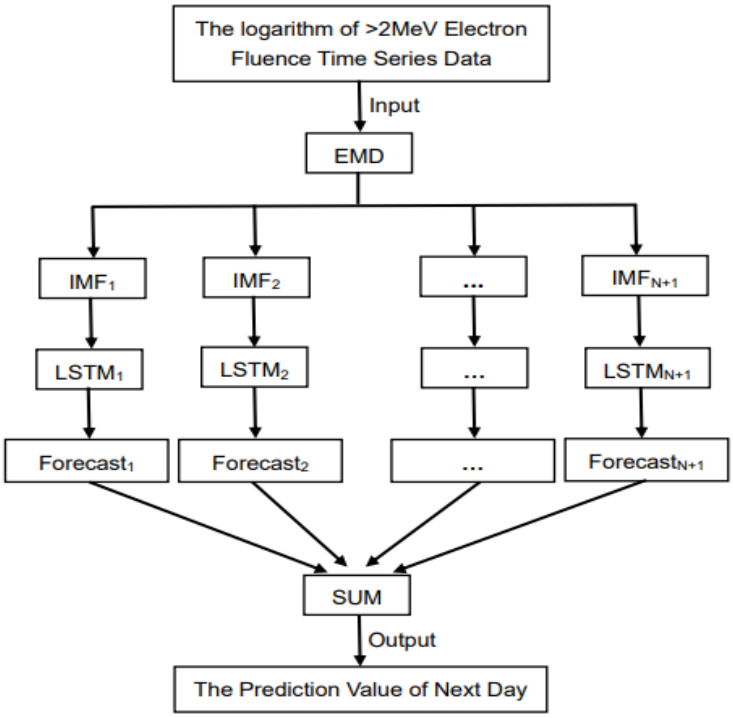

Figure 3 The flow chart of the EMD-LSTM model

4. Results and Analysis

4.1 The Evaluation of Forecasting >2MeV Electron Fluxes

In this work, we use three indicators, like Root Mean Square Error(σ), Correlation Coefficient (R), and the Prediction Efficiency(PE), to evaluate the performance of the >2 MeV electron fluxes forecasting. In the experiments, we compare the performance indicators of between the EMD-LSTM model and the other classical models. They are defined as follows:

$$\sigma=\sqrt{\frac{1}{n}\sum_{i=1}^{n}(f_i-F_i)^2} \quad (1)$$

$$R=\frac{\sum_{i=1}^{n}(f_i-\bar{f})}{\sqrt{\sum_{i=1}^{n}(f_i-\bar{f})^2(F_i-\bar{F})^2}}. \quad (2)$$

$$PE = 1 - \frac{\sum_{i=1}^{n}(f_i - F_i)^2}{\sum_{i=1}^{n}(\bar{F} - F_i)^2} \quad (3)$$

Where f_i is the forecast value, F_i is the observation value, $\bar{f}$ is the mean of the forecast value, $\bar{F}$ is the mean value of the observation, and n is the number of samples. Each of these indicators evaluates the model on a different perspective. The σ indicates error and the R indicates the level of fitting between the prediction value and the observation. The PE evaluates the accuracy of the prediction of the >2 MeV electron fluxes. As such, the smaller σ, the larger R and PE, are the better the prediction performance. We compare the σ, R and PE of predicting the >2Mev electron fluxes by between the EMD-LSTM and the classical models in the next section.

4.2 The Prediction Results of the EMD-LSTM model

In this work, the data series of the >2MeV electron fluxes from 2001 to 2009 is used by the training set, and the electron fluxes from 2010 to 2013 is used by the test set. We use the seven parameters selected as the inputs of the EMD-LSTM model. Figure 4 shows the prediction results of the EMD-LSTM model during from January 2010 to December 2011 (The red line represents the prediction value of the EMD-LSTM model and the black line represents the observation of the >2MeV electron fluxes). The forecast value of the EMD-LSTM model is close to the observation of the >2MeV electron fluxes. It is worth noting that the amount of log10(electron fluxes) is even up to 8-9, the prediction values of the EMD-LSTM model is still close to the observations. There are two main reasons. Firstly, when the amount of log10(electron fluxes) is up to 8 or 9, it is often caused by the sudden acceleration of relativistic electrons which is often related to the pc5 wave (Mathie & Mann, 2000; Lam, 2017). So, in this work, we used the pc5 as one of input parameters, and the prediction results is ideal. Secondly, the LSTM network could capture the historical information to process nonlinear problems of data series, and the EMD algorithm could reduce the influence of non-stationary of data series (Qian et al., 2020). Therefore, even if the high-energy electron fluxes changes suddenly, the EMD-LSTM model can also fit the >2 MeV electron fluxes well.

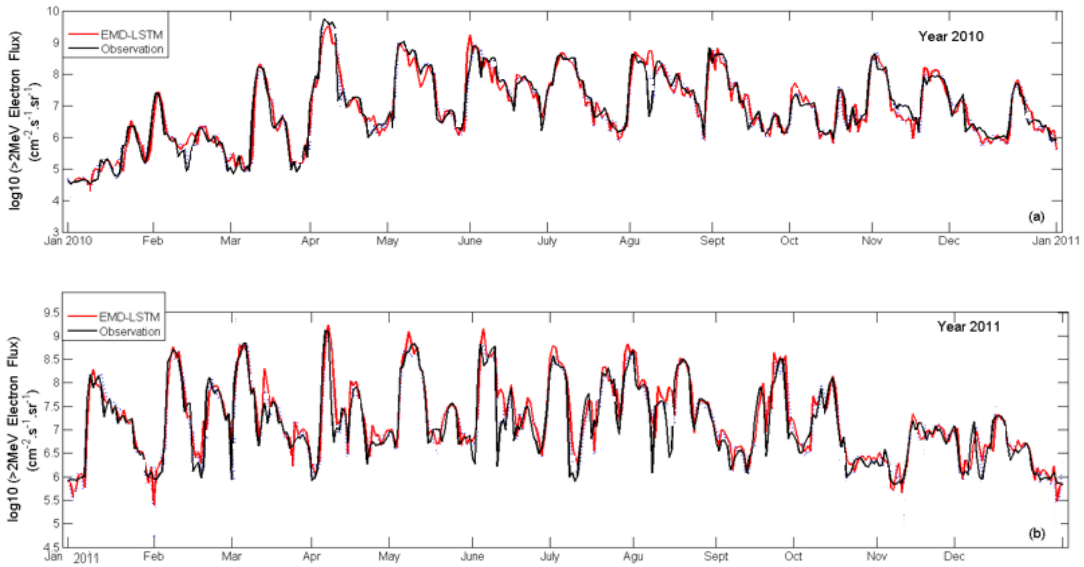

Figure 4 The comparison of the EMD-LSTM prediction values with the observations from Jan 2010 to Dec 2011.

Compared with the data sequences of the >2 MeV electron fluxes in 2010, the >2 MeV electron flux data series changes more dramatically in 2011, so the levels of non-stationary and non-linearity are significantly enhanced. The EMD-LSTM model combines the EMD algorithm effectively process the non-stationary problem of data series, with the LSTM network improves the ability of the model to deal with nonlinear problems. Comparison with the standard RNN can only remember information in a short period, the LSTM network can remember data information within a long time, and captures useful information of training set to predict the >2 MeV electron fluxes of 1 day ahead. The LSTM network can record the characteristics of the changes of the >2 MeV electron fluxes during the historical high-energy electron storms and retains the useful information. Therefore, the LSTM network can deal with sudden change of the relativistic electron fluxes events. Figure 4 shows that the EMD-LSTM model can also fit actual observation of the >2 MeV electron fluxes reaching peak values during the high-energy electron flux storm. In the actual operation, the sudden enhancement of the high-energy electron fluxes should be paid more attention to forecast, to minimize the loss by protection measures taken to the satellite equipment.

Table 3. the comparison of PE, σ and R between the EMD-LSTM and other models

Year	Model	PE	σ	R

2010	LSTM	0.89	0.37	0.94
	EMD-KLM	0.88	0.35	0.93
	EMD-LSTM	0.92	0.32	0.96
2011	LSTM	0.75	0.39	0.88
	EMD-KLM	0.77	0.41	0.89
	EMD-LSTM	0.81	0.37	0.90
2012	LSTM	0.77	0.38	0.88
	EMD-KLM	0.79	0.39	0.89
	EMD-LSTM	0.84	0.33	0.92
2013	LSTM	0.79	0.37	0.89
	EMD-KLM	0.78	0.37	0.90
	EMD-LSTM	0.83	0.34	0.92

Table 3 shows the comparison of the EMD-LSTM model with the LSTM model and the EMD-KLM model (Qian et al., 2020) based on the same datasets. The results in Table 3 indicates that the effectiveness of the EMD-LSTM model is greatly improved compared with the other two models, on the basis of the performance indicators of PE, σ and R. The data series of non-stationary and nonlinear characteristics are more obvious, which derive from the high-energy electron flux storms frequently occurs during from 2011 to 2013 especially (Qian et al., 2020). The PE of the EMD-KLM model is comparable to that of the LSTM model. Further more, the EMD-LSTM model, combined the EMD algorithm and the LSTM network, has a certain improvement in the PE compared with the other two models. This also fully shows that the EMD-LSTM model can deal with the effects of non-stationary and nonlinear characteristics, which derives from magnetic storms resulting in drastic fluctuations of the high-energy electron flux data series.

Table 4. the comparison of PE between the EMD-LSTM and the previous classical models in the period of 2003-2006

Model/Year	2003-2004	2005-2006
NICT(PE)	0.72	0.79
Low-energy(PE)	0.66	0.74

RDF(PE)	0.64	0.75
LSTM-FRK(PE)	0.74	0.81
EMD-LSTM(PE)	0.79	0.83

Table 4 shows the PE comparison of between the EMD-LSTM model and the previous classical models. It is indicates that the PEs of the EMD-LSTM model is higher than that of those models in the period of 2003-2006. Specially, the improvement of PE in 2003-2004 is the most obvious. There are 13 high-energy electron flux storm events occurred in 2003-2004, more than double times in 2005-2006. Therefore, the variation of the >2 MeV electron fluxes in 2003-2004 is more drastic, and the level of non-stationary and nonlinear of the data series is significantly enhanced. So, the PEs of all prediction models in 2003- 2004 is lower than that in 2005-2006. The EMD-LSTM model can deal with the non-stationary and nonlinear problems of data series well by the improvement of mathematical method. Therefore, even in the year with strong non-stationary and nonlinear level, the EMD-LSTM model can also achieve better PE performance. In addition, the most of models (Li et al., 2001; Turner and Li, 2008; Wei et al., 2018) in Table 4, used solar wind as input parameters, but the EMD-LSTM model uses Pc5 and related geomagnetic indexes to forecast the >2 MeV electron fluxes . On the basis of the experimental results, it is found that geomagnetic pulsation parameters can also achieve a better forecast effect as a forecasting factor of the model. The prediction results of the EMD-LSTM model also verify the feasibility of geomagnetic pulsation parameter as a predictor of high-energy electron fluxes.

4.3 Analysis of the >2 MeV Electron Fluxes During Magnetic Storms

During a geomagnetic storm, the high-energy electron fluxes changes dramatically, so the accurate prediction of the >2 MeV electron fluxes is very important to protect for satellite instruments to reduce the risk of damage. Here, two cases of the high-energy electron flux storm, during from 16 July to 25 July 2012 and from 28 May to 6 June 2013, are chose to analysis. The prediction results is illustrated in Figure 5. During an initial phase of magnetic storm, the >2 MeV electron fluxes will decrease greatly and then rise rapidly, which is consistent with the variation characteristics of the general electron flux storms. Specially, the extreme points of the data series, on 20 July 2012 and 1 June 2013, are very important to the

prediction, which indicate the high-energy electron fluxes begins to rapidly enhance. As can be seen in Figure 5, the prediction values of the EMD-LSTM model is consistent with the observation of the >2 MeV electron fluxes, and particularly the prediction values coincide with the observation values at the extreme points, few time offset.

There are two reasons for highly effective in prediction. Firstly, the EMD algorithm greatly reduces the non-stationary problem caused by the drastic changes of the high-electron fluxes (Qian, et al., 2020). Secondly, the LSTM network can remember the variation characteristics of the high-energy electron storm events in the training set and extract the relevant information (Wei et al., 2018). Therefore, when the high-energy electrons suddenly drop, the LSTM network can accurately predict the subsequent values of the >2 MeV electron fluxes, based on the analysis of the information of the training set samples. This is very important in practical forecasting, to accurately predict the start time of high-energy electron storm and provide immediate protection for satellite equipment.

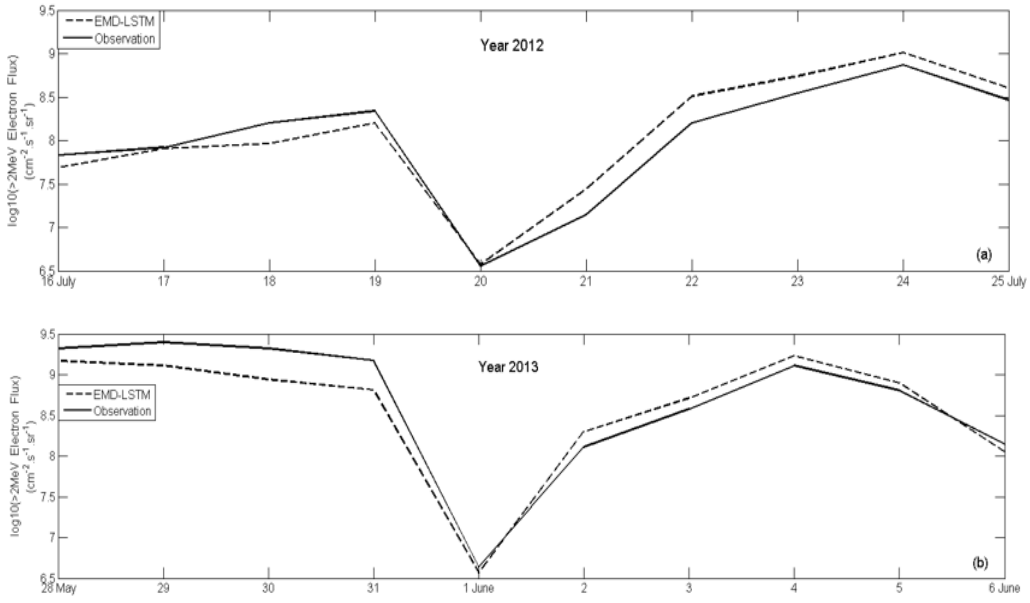

Figure 5. The comparison of the EMD-LSTM model prediction with the observations during energy electron storm events

5. Conclusion

In this paper, we combine the EMD algorithm and the LSTM network to construct the EMD-LSTM model to predict the > 2MeV electron fluxes at GEO. The EMD-LSTM model can deal with the non-stationary and nonlinear of data series, and the effectiveness of the

model is improved compared with other classical models.

The prediction results of the EMD-LSTM model is excellent during the high-energy electron fluxes storm, and particularly the extreme points of the >2 MeV electron fluxes data series is accurately predicted, and few time offset.

Pc5 and related geomagnetic indexes are used to predict the > 2MeV electron fluxes. The experimental results verify that the parameters of ground can achieve a better forecast effect as a forecasting factor of the model, and those data acquisition of parameters is stable and lower cost.

Acknowledgments: This work was supported by the National Key R&D Program of China (2018YFF01013706), the Natural Science Foundation of Jiangsu Province (BK20170952), the National Natural Science Foundation of China grant (No.41874190, 42074183, 61572015), and the Stable support projects of institutes for basic scientific research (A131901W14). The author acknowledges National Oceanic and Atmospheric Administration(NOAA), NASA OMNI database and the Word Data center for Geomagnetism, Kyoto for providing the observation data.

Data Availability Statement:

The high-energy electron fluxes observations originates from the GOES satellite on the website of NOAA (https://satdat.ngdc.noaa.gov/sem/goes/data). Geomagnetic indexes come from the world geomagnetic data center of the Memanbetsu station in Japan (http://swdcwww.kugi.kyoto-u.ac.jp/wdc/Sec3.html). The daily Pc5 power datasets derives from ground magnetic data, which is collected by CANMOS observatories.

References

Baker, D. N., Mcpherron, R. L., Cayton, T. E., & Klebesadel, R. W. (1990). Linear prediction filter analysis of relativistic electron properties at 6.6 RE. Journal of Geophysical Research: Space Physics, 95, 15133-15140. https://doi.org/10.1029/JA095iA09p15133.

Borovsky, J. E., & Denton M. H. (2014). Exploring the cross correlations and autocorrelations of the ULF indices and incorporating the ULF indices into the systems science of the solar wind-driven magnetosphere. Journal of Geophysical Research: Space Physics, 119, 4307 -4334. doi:10.1002/2014JA019876.

Futaka, M., Taguchi, S., Okuzawa, T., & Obara, T. (2002). Neural network prediction of relativistic electrons at geosynchronous orbit during the storm recovery phase: effects of recurring substorms. Annales Geophysicae, 20, 947-951. doi: 10.5194/angeo-20-947-200 2.

Graves, A. (2012). Long Short-Term Memory. Springer Berlin Heidelberg, 37-45. doi: 10.100 7/978-3-642-24797-2_4.

Guo, C., Xue, B. S., & Lin, Z. X. (2013). Geosynchronous orbit high energy electron flux prediction method. Chinese Journal of space science, 33 (4), 418-426.

He, T., Liu, S. Q., Shen, H., & Gong, J. C. (2013). Quantitative prediction of relativistic electron flux at geosynchronous orbit with geomagnetic pulsations parameters. Chinese Journal of space science, 33(1), 20-27.

Hochreiter, S., & Schmidhuber, J. (1997). Long Short-Term Memory. Neural Computation, 9(8), 1735-1780. doi:10.1162/neco.1997.9.8.1735.

Huang, N. E., Shen, Z., & Long, S. R. (1998). The empirical mode decomposition and the Hilbert spectrum for nonlinear and non-stationary time series analysis. Proceedings of The Royal Society of London A: Mathematical, Physical and Engineering Sciences, 454(1971):903-995. https://doi.org/10.1098/rspa.1998.0193.

Lam, H.-L. (2017). On the predictive potential of Pc5 ULF waves to forecast relativistic electrons based on their relationships over two solar cycles. Space Weather, 15, 163-179. doi:10.1002/2016SW001492.

Li, X., Termerin, M., Baker, D. N., Reeves, G. D., & Larson, D. (2001). Quantitative prediction of radiation belt electrons at geostationary orbit based on solar wind measurements. Geophysical Research Letters, 28(9). https://doi.org/10.1029/2000GL0126 81.

Ling, A. G., Ginet G. P., Hilmer, R. V., & Perry, K. L. (2010). A neural network-based geosynchronous relativistic electron flux forecasting model. Space Weather, 8, S09003. doi:10.1029/2010SW000576.

Mathie, R. A., & Mann, I. R. (2000). A correlation between extended intervals of ULF wave power and storm-time geosynchronous relativistic electron flux enhancements. Geophysical Research Letters,27(20), 3261-3264. doi:10.1029/2000GL003822.

O'Brien, T. P., Lorentzen, K. R., Man, I. R., Meredith, N. P., Blake, J. B., Fennell, J. F.,

Looper, M. D., Milling, D. K., & Anderson, R. R. (2003). Energization of relativistic electrons in the presence of ULF power and MeV microbursts: Evidence for dual ULF and VLF acceleration. Journal of Geophysical Research, 108(A8), 1329. doi:10.1029/2002JA009784.

Potapov, A., Ryzhakova, L., & Tsegmed, B. (2016). A new approach to predict and estimate enhancements of “killer” electron flux at geosynchronous orbit. Acta Astronautica, 126, 47-51. http://dx.doi.org/10.1016/j.actaastro.2016.04.017.

Potapov, A., Tsegmed, B., & Ryzhakova, L. (2014). Solar cycle variation of “killer” electrons at geosynchronous orbit and electron flux correlation with the solar wind parameters and ULF waves intensity. Acta Astronautica, 93, 55–63. https://doi.org/10.1016/j.actaastro.2013.07.004.

Qian, Y. D., Yang, J. W., Zhang, H., Shen, C. & Wu, Y. (2020). An hourly prediction model of relativistic electrons based on empirical model decomposition. Space Weather, 17, e2018SW0022078. https://doi.org/10.1029/2018SW002078.

Regi, M., Lauretis, M., & Francia, P. (2015). Pc5 geomagnetic fluctuations in response to solar wind excitation and their relationship with relativistic electron fluxes in the outer radiation belt. Earth, Planets and Space, 67, 1-9. http://doi.org/10.1186/s40623-015-0180-8.

Sain, & Stephan, R. (1997). The nature of statistical learning theory. Technometrics, 38(4),409-422. doi:10.1080/00401706.1996.10484565.

Sakaguchi, K., Miyoshi, Y., Satio, S., Nagatsuma, T., Seki, K., & Murata, K. T. (2013). Relativistic electron flux forecast at geostationary orbit using Kalman filter based on a multivariate autoregressive model. Space Weather, 11, 79-89. doi:10. 1002/swe.20020.

Simms, L., Engebretson, M., Clilverd, M., Rodger, C., Lessard, M., Gjerloev, J., & Reeves, G. (2018). A distributed lag Autoregressive model of geostationary relativistic electron fluxes: comparing the influences of waves, seed and source electrons and solar wind inputs. Journal of Geophysical Research:Space Physics, 123, 3646-3671. https://doi.org/10.1029/2017JA025002.

Tan, Y., Hu, Q., Wang, Z., & Zhong, Q. (2018). Geomagnetic index Kp forecasting with LSTM. Space Weather, 16, 406-416. https://doi.org/10.1002/2017SW001764.

Turner, D. L., & Li, X. (2008). Quantitative forecast of relativistic electron flux at

geosynchronous orbit based on low-energy electron flux. Space Weather, 6, S05005. doi:10.1029/2007SW000354.

Wei, L., Zhong, Q., Lin, R., Wang, J., Liu, S., & Cao, Y. (2018). Quantitative prediction of high-energy electron integral flux at geostationary orbit based on deep learning. Space Weather, 16, 903–916. https://doi.org/10.1029/2018SW001829.

Wrenn, G. L., Rodgers, D. J., & Ryden, K. A. (2002). A solar cycle of spacecraft anomalies due to internal charging. Annales Geophysicae, 20, 953-956. https://doi.org/10.5194/angeo-20-953-2002.

Xiao, F. L., Zhang, S., Su, Z., He, Z., &Tang, L. (2012). Rapid acceleration of radiation belt energetic electrons by Z-mode waves. Geophysical Research Letters, 39, L03103. doi:10.1029/2011GL050625.

Xue, B. S., & Ye, Z. (2004). Method for forecasting relativistic electron enhancement events in geosynchronous orbit. Chinese Journal of Space Science, 24 (4), 283-288.

Yousrfi, M. R., Kasmaei, B. S., Vahabie, A.,Lucas, C., & Araabi, B. N. (2009). Input selection based on information theory for constructing predictor models of solar and geomagnetic activity indices. Solar Physics, 258(2), 297-318. https://doi.org/10.1007/s11207-009--9418-6.

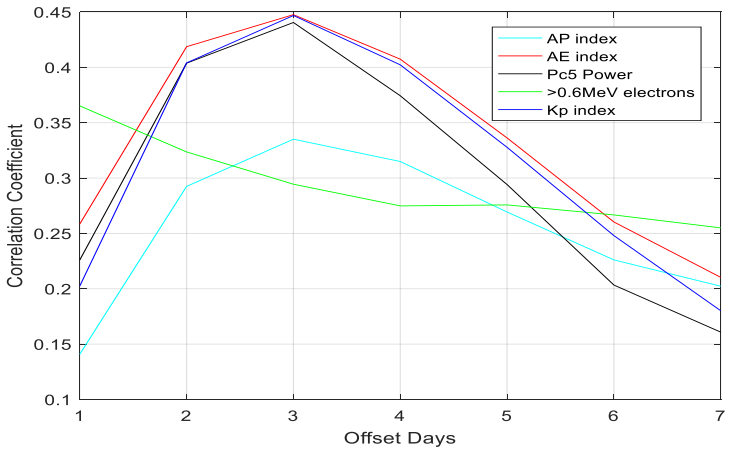

Figure1. The correlations of between input parameters used and >2MeV electron fluxes.

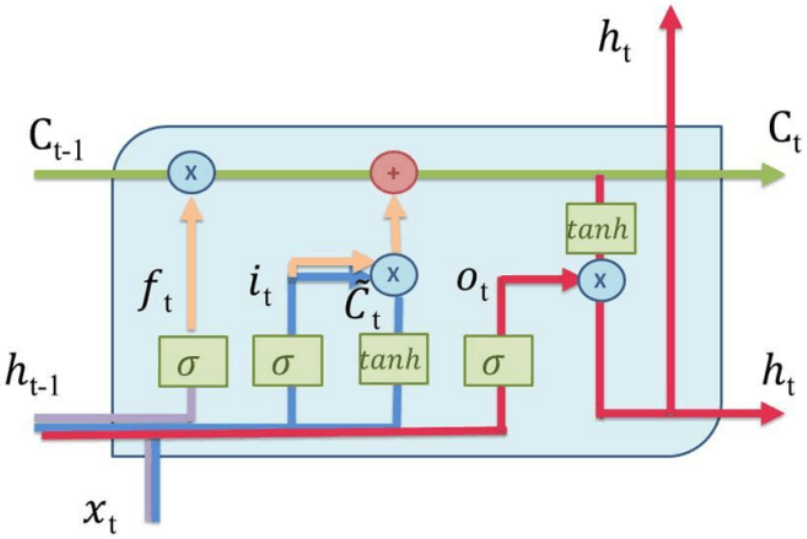

Figure 2. LSTM cell of schematic diagram. The cell state is in green, the forget in purple, the input gate in blue, and the output gate in red.

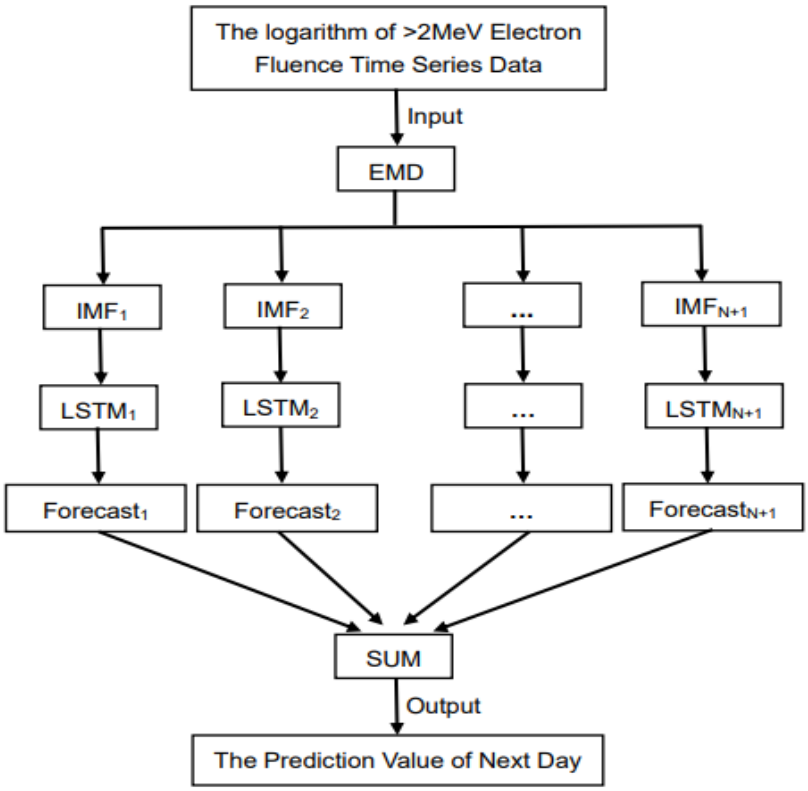

478

479 Figure 3. The flow chart of the EMD-LSTM model

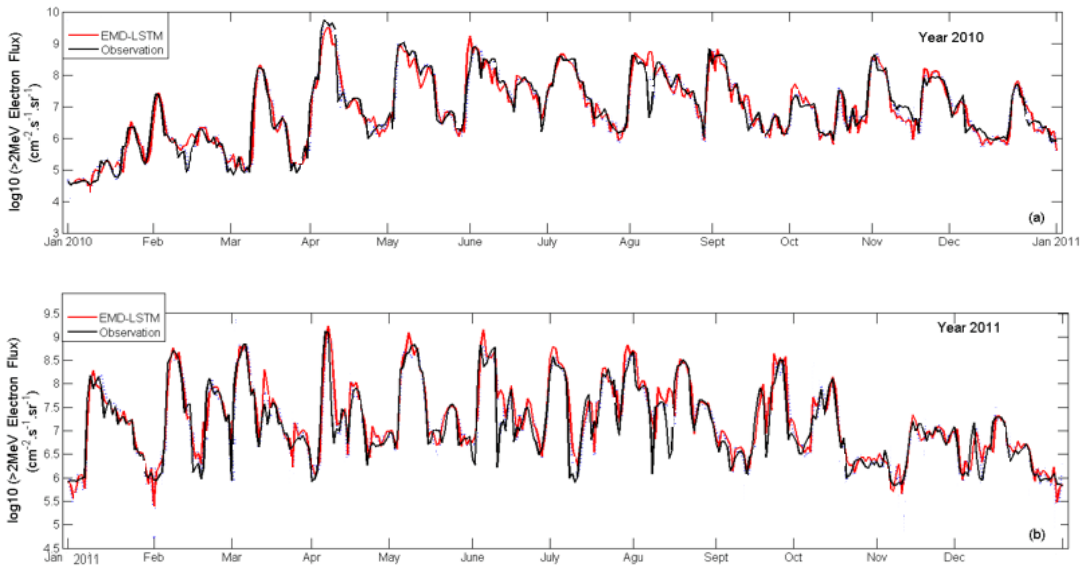

480

481

482 Figure 4. The comparison of the EMD-LSTM prediction values with the observations from

483 Jan 2010 to Dec 2011.

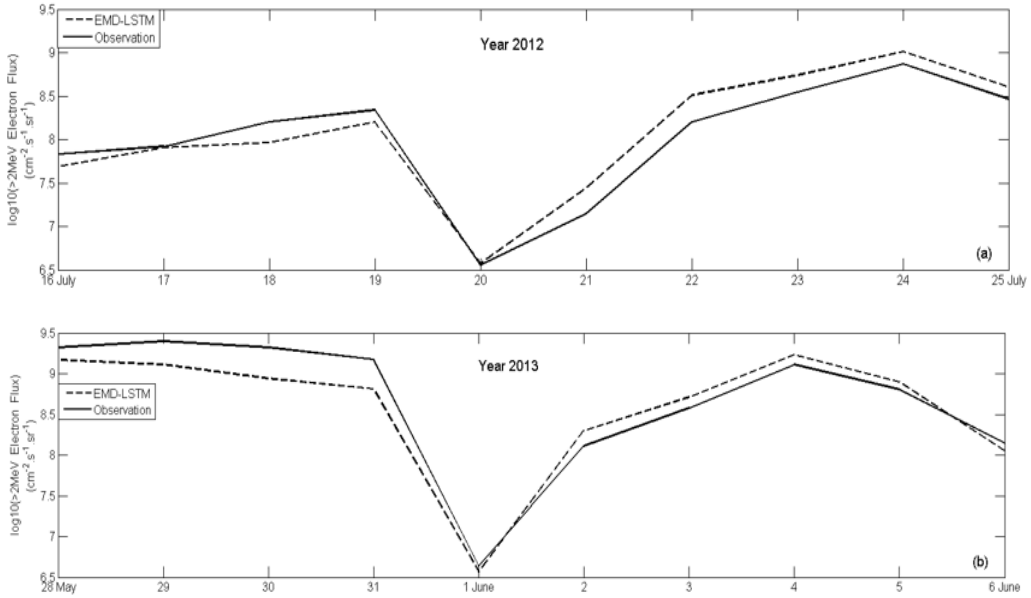

Figure 5. The comparison of the EMD-LSTM model prediction with the observations during energy electron storm events.

Table1. Coordinates of CANMOS Auroral Zone Observatories.

Code	Station	Geographic Latitude	Geographic Longitude	Geomagnetic Latitude	Geomagnetic Longitude	L
FCC	ForChurchill	$58.8^{\circ}N$	$94.1^{\circ}W$	$68.8^{\circ}N$	$94.1^{\circ}W$	8.18

Table2. The input parameters of the EMD-LSTM model.

Inputs	Correlation coefficient
$Ap(t-3)$	0.33
$AE(t-3)$	0.46
$>0.6MeV(t-1)$	0.36
$Pc5(t-3)$	0.43
$Pc5(t-2)$	0.40

$Kp(t-3)$	0.44
$X(t-1)$	0.81

Table 3. the comparison of PE, σ and R between the EMD-LSTM and other models.

Year	Model	PE	σ	R
2010	LSTM	0.89	0.37	0.94
	EMD-KLM	0.88	0.35	0.93
	EMD-LSTM	0.92	0.32	0.96
2011	LSTM	0.75	0.39	0.88
	EMD-KLM	0.77	0.41	0.89
	EMD-LSTM	0.81	0.37	0.90
2012	LSTM	0.77	0.38	0.88
	EMD-KLM	0.79	0.39	0.89
	EMD-LSTM	0.84	0.33	0.92
2013	LSTM	0.79	0.37	0.89
	EMD-KLM	0.78	0.37	0.90
	EMD-LSTM	0.83	0.34	0.92

Table 4. the comparison of PE between the EMD-LSTM and the previous classical models in the period of 2003-2006.

Model/Year	2003-2004	2005-2006
NICT(PE)	0.72	0.79
Low-energy(PE)	0.66	0.74
RDF(PE)	0.64	0.75
LSTM-FRK(PE)	0.74	0.81
EMD-LSTM(PE)	0.79	0.83